

Werk

Jahr: 1986

Kollektion: fid.geo

Signatur: 8 Z NAT 2148:59

Werk Id: PPN1015067948_0059

PURL: http://resolver.sub.uni-goettingen.de/purl?PID=PPN1015067948_0059 | LOG_0020

Terms and Conditions

The Goettingen State and University Library provides access to digitized documents strictly for noncommercial educational, research and private purposes and makes no warranty with regard to their use for other purposes. Some of our collections are protected by copyright. Publication and/or broadcast in any form (including electronic) requires prior written permission from the Goettingen State- and University Library.

Each copy of any part of this document must contain there Terms and Conditions. With the usage of the library's online system to access or download a digitized document you accept the Terms and Conditions.

Reproductions of material on the web site may not be made for or donated to other repositories, nor may be further reproduced without written permission from the Goettingen State- and University Library.

For reproduction requests and permissions, please contact us. If citing materials, please give proper attribution of the source.

Contact

Niedersächsische Staats- und Universitätsbibliothek Göttingen
Georg-August-Universität Göttingen
Platz der Göttinger Sieben 1
37073 Göttingen
Germany
Email: gdz@sub.uni-goettingen.de

A comparison of upper mantle subcontinental electrical conductivity for North America, Europe, and Asia

Wallace H. Campbell¹ and Edward R. Schiffmacher²

¹ U.S. Geological Survey, MS 964, Box 25046, Denver Federal Center, Denver, CO 80225, USA

² 2155 Emerald Road, Boulder, CO 80303, USA

Abstract. Spherical harmonic analysis coefficients of the external and internal parts of the quiet-day geomagnetic field variations (Sq), separated for the North American, European, Central Asian and East Asian regions, were used to determine conductivity profiles to depths of about 600 km by the Schmucker equivalent-substitute conductor method. All three regions showed a roughly exponential increase of conductivity with depth. Distinct discontinuities seemed to be evident near 255–300 km and near 450–600 km. Regional differences in the conductivity profiles were shown by the functional fittings to the data. For depths less than about 275 km, the North American conductivities seemed to be significantly higher than the other regions. For depths greater than about 300 km, the East Asian conductivities were largest.

Key words: Upper mantle – Electrical conductivity – Electromagnetic induction

Introduction

In an earlier paper (Campbell and Schiffmacher, 1985) a Gauss spherical harmonic analysis (SHA) technique was applied to quiet-day geomagnetic variation (Sq) data to separate the external and internal contributions of the observed magnetic field at the Earth's surface. A hypothetical sphere was used to determine the separation for restricted regions of the Earth, so that equivalent ionosphere source currents were found individually for North America, Europe, Central Asia and East Asia. The field at any geomagnetic colatitude, θ , and longitude, ϕ , within the continental study region, was represented by ordered sets of spherical harmonic analysis (SHA) external cosine, $(aex)_n^m$, and sine, $(bex)_n^m$, coefficients and internal cosine, $(ain)_n^m$, and sine, $(bin)_n^m$, coefficients. The order index, m , was equal to 1, 2, 3, or 4 for the 24-, 12-, 8- and 6-h components of the quiet daily variation, Sq, and the analysis was computed with degree indices, n , equal to m to 12. The three orthogonal field components in the geomagnetic northward, X ,

eastward, Y , and downward, Z , directions were represented by the expressions:

$$X(\theta, \phi) = \sum_{m=1}^4 \sum_{n=m}^{12} \{ [(aex)_n^m + (ain)_n^m] \cos(m\phi) + [(bex)_n^m + (bin)_n^m] \sin(m\phi) \} \frac{dP_n^m}{d\theta}, \quad (1)$$

$$Y(\theta, \phi) = \sum_{m=1}^4 \left(\frac{-m}{\sin \theta} \right) \sum_{n=m}^{12} \{ [(bex)_n^m + (bin)_n^m] \cos(m\phi) - [(aex)_n^m + (ain)_n^m] \sin(m\phi) \} P_n^m, \quad (2)$$

$$Z(\theta, \phi) = \sum_{m=1}^4 \sum_{n=m}^{12} \{ [n(aex)_n^m - (n+1)(ain)_n^m] \cos(m\phi) + [n(bex)_n^m - (n+1)(bin)_n^m] \sin(m\phi) \} P_n^m, \quad (3)$$

where P_n^m is the Schmidt Normalized Associated Legendre function (Chapman and Bartels, 1940).

In the application of SHA coefficients to earth conductivity determinations, Schmucker (1970, 1979) showed that for any specified n and m the ratio of the vertical, $(Z)_{n,m}$, to one of the horizontal field components, $(X)_{n,m}$ or $(Y)_{n,m}$, determines a complex transfer function, C_n^m , in kilometres such that

$$C_n^m = \left[\frac{R(dP_n^m/d\theta)}{n(n+1)P_n^m} \right] \frac{(Z)_{n,m}}{(X)_{n,m}} \quad (4)$$

and

$$C_n^m = i \left[\frac{-mR}{n(n+1)\sin \theta} \right] \frac{(Z)_{n,m}}{(Y)_{n,m}}, \quad (5)$$

where R is the earth's radius in kilometres. Writing this function in the complex real (z) and imaginary ($-p$) form

$$C_n^m = z - ip \quad (6)$$

he was able to determine the earth's electrical response to the penetrating fields using uniform substitute conducting layers at depths determined by the transfer function.

Campbell and Anderssen (1983) showed that the real and imaginary parts of this transfer function may be written directly in terms of the SHA coefficients:

$$z = \frac{R}{n(n+1)} \left\{ \frac{A_n^m [n(\text{aex})_n^m - (n+1)(\text{ain})_n^m] + B_n^m [n(\text{bex})_n^m - (n+1)(\text{bin})_n^m]}{(A_n^m)^2 + (B_n^m)^2} \right\} \quad (7)$$

and

$$p = \frac{R}{n(n+1)} \left\{ \frac{A_n^m [n(\text{bex})_n^m - (n+1)(\text{bin})_n^m] - B_n^m [n(\text{aex})_n^m - (n+1)(\text{ain})_n^m]}{(A_n^m)^2 + (B_n^m)^2} \right\}, \quad (8)$$

where z and p are given in kilometres and the coefficient sums are given by

$$A_n^m = [(\text{aex})_n^m + (\text{ain})_n^m] \quad \text{and} \quad B_n^m = [(\text{bex})_n^m + (\text{bin})_n^m]. \quad (9)$$

For each m, n set of coefficients the depth to the uniform substitute layer is given by

$$d_{n,m} = z - p \text{ (km)} \quad (10)$$

with a substitute-layer conductivity of

$$\sigma_{n,m} = 5.4 \times 10^4 / m (\pi p)^2 \quad (\text{siemens/meter}). \quad (11)$$

The ratio, S_n^m , of the internal to external components of the geomagnetic surface field is then

$$S_n^m = u + i v \quad (12)$$

where

$$u = \frac{(\text{aex})_n^m (\text{ain})_n^m + (\text{bex})_n^m (\text{bin})_n^m}{[(\text{aex})_n^m]^2 + [(\text{bex})_n^m]^2} \quad (13)$$

and

$$v = \frac{(\text{bex})_n^m (\text{ain})_n^m - (\text{aex})_n^m (\text{bin})_n^m}{[(\text{aex})_n^m]^2 + [(\text{bex})_n^m]^2}. \quad (14)$$

The validity of Eqs. (10) and (11) is limited by three conditions. The first of these is:

$$0^\circ \leq \arg(C_n^m) \leq -45^\circ, \quad (15)$$

a condition described by Schmucker (1979). The second is

$$\arg(S_n^m) \geq 9^\circ, \quad (16)$$

a requirement that the angle between the internal and external components be neither small nor negative. The third condition is that the SHA amplitudes (Eq. 9) are not small:

$$[(A_n^m)^2 + (B_n^m)^2]^{0.5} \geq G_m. \quad (17)$$

A study of the data samples showed that sufficient sizes of the low-amplitude exclusion factors, in gamma, are $G_1 = 1.5$, $G_2 = 1.0$, $G_3 = 0.5$ and $G_4 = 0.25$, in a ratio of 1:2/3:1/3:1/6. The shorter wavelength, higher m , components of the field are typically smaller in amplitude. This ratio is approximately the same as that of the averaged amplitudes of the 24-, 12-, 8- and 6-h

Fourier components of the Sq field at each 2.5-degree latitude increment weighted by the cosine of latitude.

This paper uses the coefficients from the earlier spherical harmonic analysis of Sq fields in North America, Europe, Central Asia and East Asia to determine the equivalent conductivity profiles beneath these three continental regions, by applying the Schmucker (1970, 1979) technique with the above equations.

Analysis

The original data set for this determination comprised the Sq variations on exceptionally quiet days of the quiet-sun year, 1965. Figure 1 shows the locations of the thirty observations used for the study. Spherical harmonic representations of the field variations for the 7th and 21st day of each month were obtained with the analysis sequence outlined in the earlier paper (Campbell and Schiffmacher, 1985). This sequence was used to form a regional station representation of the three orthogonal field components of Sq from the 24-, 12-, 8- and 6-h Fourier coefficients together with their seasonal (annual and semiannual) changes. The Fourier coefficients were appropriately smoothed with respect to geomagnetic latitude, and then the SHA technique was used on 2.5°-latitude samples to obtain the Gauss coefficients $(\text{aex})_n^m$, $(\text{bex})_n^m$, $(\text{ain})_n^m$, and $(\text{bin})_n^m$ for order 4 and degree 12. The analysis procedure was applied to each region separately with the local time change of field made equivalent to longitude position and the southern hemisphere field modelled appropriately from that of the northern observatory region. This analytical method was roughly equivalent to the creation of a sphere surrounded by a unique-source current pattern and having an internal, spherically symmetrical, conductivity-depth profile that was representative of the grouped stations of the study region. Figure 2 shows the internal induced currents obtained by the SHA. The corresponding external-source current representations were given in the earlier paper (Campbell and Schiffmacher, 1985).

The 24 sets of internal and external SHA coefficients (two for each month) calculated for each region of the model provided the input to the above equations. Conductivity-depth values were determined and plotted as separate regional data sets (Fig. 3). A trial exponential curve was fitted (by least squares) separately for each data set, after excluding a few obvious outliers, and a histogram was drawn for the distribution of data points about each trial curve. Often, the distribution was bimodal and a further separation of the data could be made for a depth of about 250–300 km. In these cases, a second exponential curve was

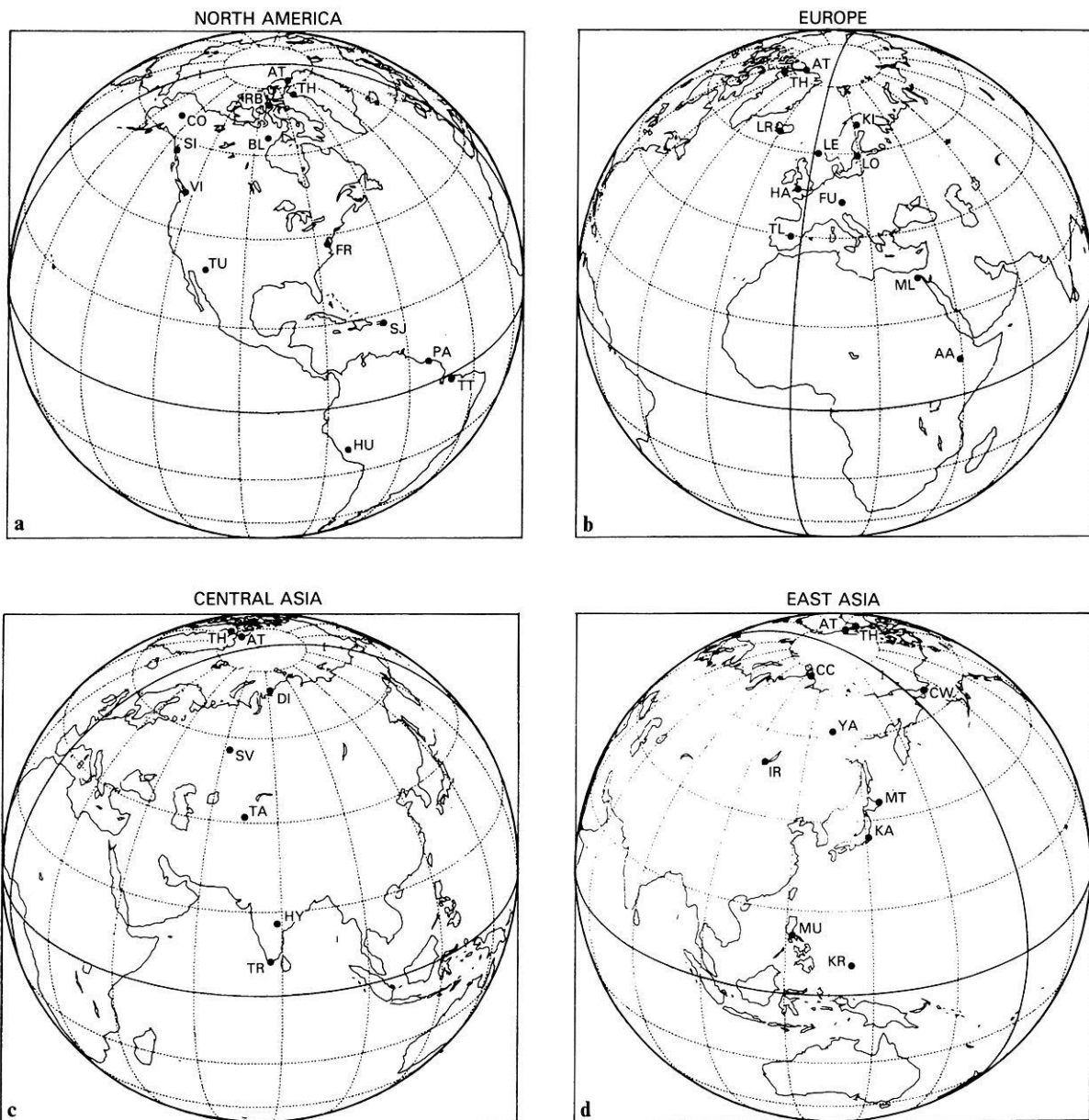


Fig. 1 a–d. Map of four analysis regions showing location of geomagnetic observatories used in the spherical harmonic analysis of the quiet-day records for **a** North America, **b** Europe, **c** Central Asia, **d** East Asia. (Station names and coordinates are given in Campbell and Schiffmacher, 1985.)

fitted to each of the new, more limited data sets, and further histograms were drawn to determine the distribution of the points about these curves. Values at the tails of the histograms were excluded and final determinations made of the best exponential representations of the data sets. Table 1 and Fig. 4 give the exponential depth-conductivity functions for the four regions after the exclusion of points at the distribution tails. Figure 5 shows the data points remaining after exclusion of distribution tails about the exponentials of Fig. 4.

Discussion

Although the results all indicated a general exponential increase of conductivity with depth from about 30–

650 km, slightly different distributions of the values were obtained for the separate regions. In addition, there seemed to be some evidence for discontinuities near 225–300 km and near 450–600 km. These locations are near phase change depths identified on seismic records (Dziewonski and Anderson, 1981). At depths less than about 275 km the North American conductivity seemed to be significantly higher than that of the other three regions. At depths greater than about 275 km there seemed to be a bifurcation of the East Asian values, a main branch providing slightly greater conductivities than the other two regions and a minor branch with lower conductivities.

Most previous determinations of deep earth conductivity (c.f. Banks, 1969; Lahiri and Price, 1939) used the global data in such a way that an average, spheri-

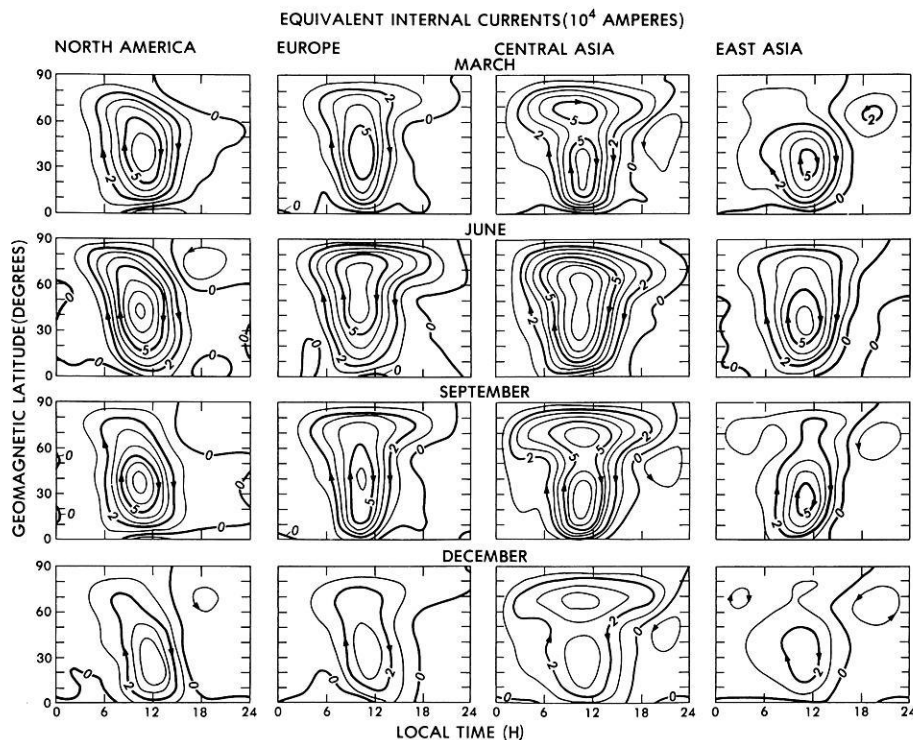


Fig. 2. Equivalent internal induced current for Sq daily variations of field in continental regions of North America (first column), Europe (second column), Central Asia (third column) and East Asia (fourth column). Examples for the four selected months of March, June, September and December are given in the top to bottom rows respectively. Each pattern in local-time versus latitude coordinates shows the equivalent current contours in 10^4 -A steps with arrows for the required flow direction. A midnight zero current level was assumed

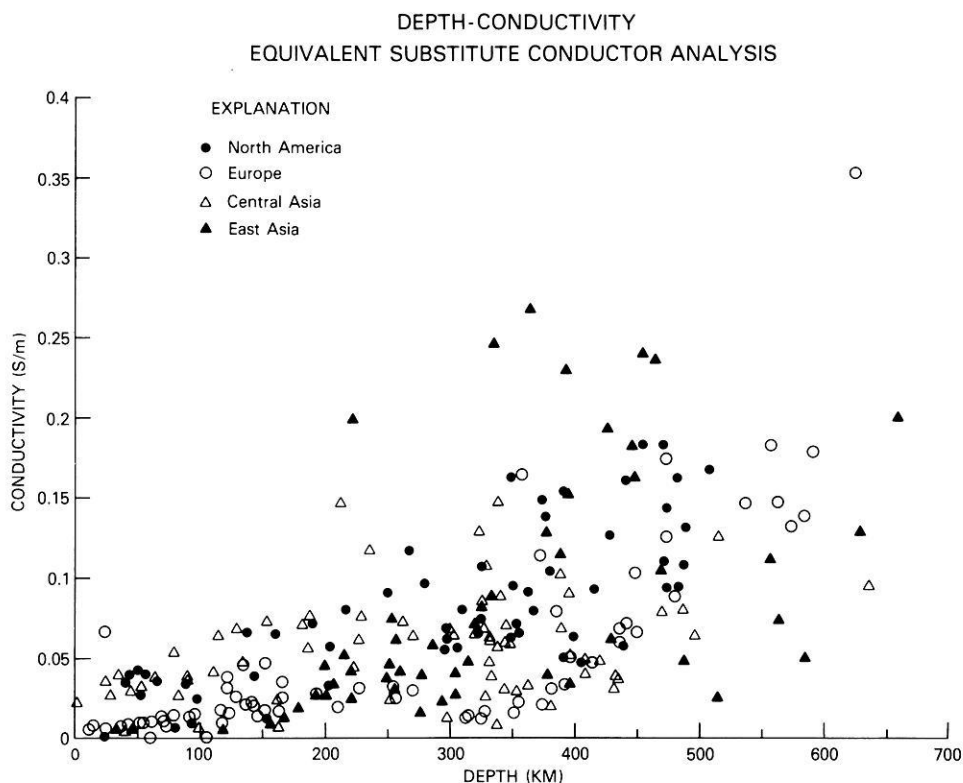


Fig. 3. Depth-conductivity values from Eqs. (10) and (11) obtained by application of the spherical harmonic analysis coefficients to Eqs. (7) and (8). The evaluations are separated for the North American, European, Central Asian and East Asian regions

cally symmetric profile was obtained. The method presented here shows some separation of regions, with slightly differing distributions of conductivity beneath the three continental regions. The large differences in the source and induced currents of the three regions justify the regional separation in the analysis. If the

observatory data of all three regions had been included in a single analysis a conductivity profile close to the mean distribution of all the points in Fig. 5 would have been obtained.

We would like to assume that the differences in the exponential curves of Fig. 4 represent the differences in

Table 1. Exponential representations of conductivity

Region	Approx. depth d (km)	Conductivity σ (s/m)
North America	30–275	$0.031 \exp(0.0045d)$
	275–500	$0.027 \exp(0.0032d)$
Europe	10–275	$0.0097 \exp(0.0052d)$
	275–620	$0.0012 \exp(0.0089d)$
Central Asia	20–300	$0.033 \exp(0.0032d)$
	300–640	$0.041 \exp(0.0011d)$
East Asia	30–475	$0.0049 \exp(0.0085d)$
	275–650	$0.0049 \exp(0.0053d)$

conductivity beneath the three regions. The problem, of course, is that the stations used to sample each region are located over a variety of upper mantle conditions. Certainly, because the analysis excluded low amplitude values and removed distribution outliers, those parts of a region beneath the more intense source currents and those stations above similar conductivity profiles are emphasized in the results.

The electrical conductivity, σ , of the multiphase silicates expected to exist in the upper mantle is thought to vary with the temperature, T , roughly as

$$\sigma = Ce^{-D/T}, \quad (18)$$

where C and D are constants for the average characteristics at a given depth (Shankland and Waff, 1977). Thus, for a given composition and principal phase of the silicates in the upper mantle, as the temperature increases with depth the conductivity also increases. In

regions of thin crust, where upper mantle magma is closest to the surface, measurements of the heat flow have larger values. Pollack and Chapman (1977) published global heat-flow contours and related this information to the thickness of the earth's lithosphere. The conductivity profiles of the first few hundred kilometres should show lower values for thicker lithospheres (or lower heat-flow values). Taking those several stations not too far from the Sq current focus as the significant ones, it seems to us that Pollack and Chapman's (1977) lithosphere is thinner beneath the North American group than the other three groups, justifying the differences in conductivity profiles that we found down to about 275 km. However, the lithospheric differences are not very clear.

Anderson and Dziewonski (1984) used a seismic tomography technique to map the earth's mantle in three dimensions. They identified large-scale convective heat-flow patterns beneath the continental regions, which would produce regional electrical conductivity differences of the type shown in Fig. 5.

It is also possible that the two branches of the East Asia profile below 275 km show the effect of the subducting oceanic slab on the important stations of that region, but certainly this cannot be confirmed at present.

In summary, Schmucker's (1970, 1979) method of determining effective depth and conductivity was applied to data from four separated continental regions. In all cases the conductivity increased exponentially with depth. There appeared to be distinct discontinuities near 225–300 km and near 450–600 km, and there were significant differences in conductivity profiles for the four regions. Although the differences seemed real, they could not be simply explained because

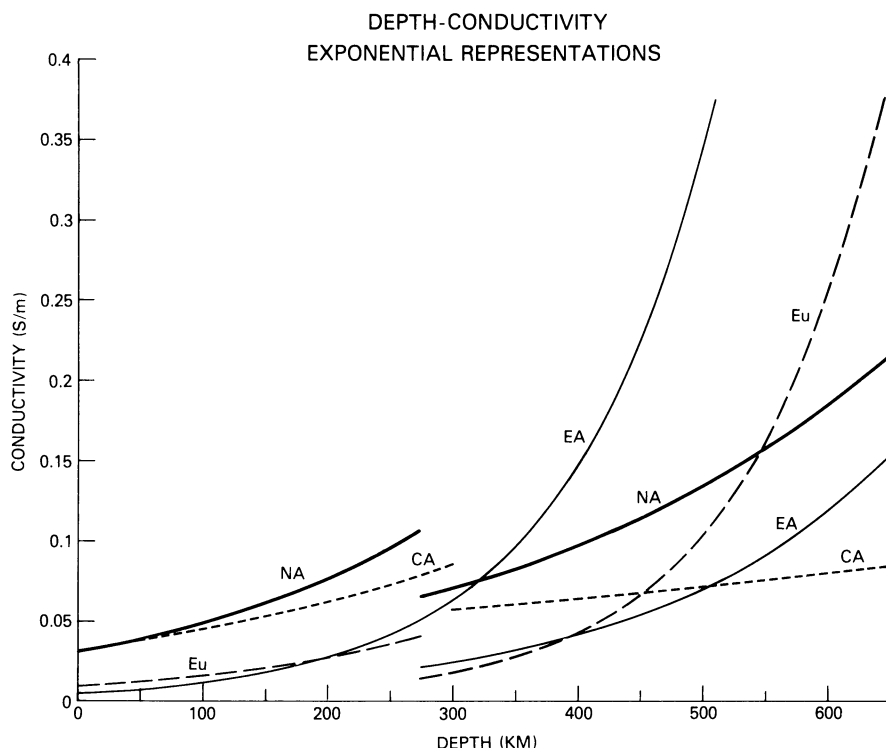


Fig. 4. Best exponential representations of depth-conductivity data given in Fig. 3. Separate curves are shown for North America (NA), Europe (Eu), Central Asia (CA) and East Asia (EA). The functions are listed in Table 1

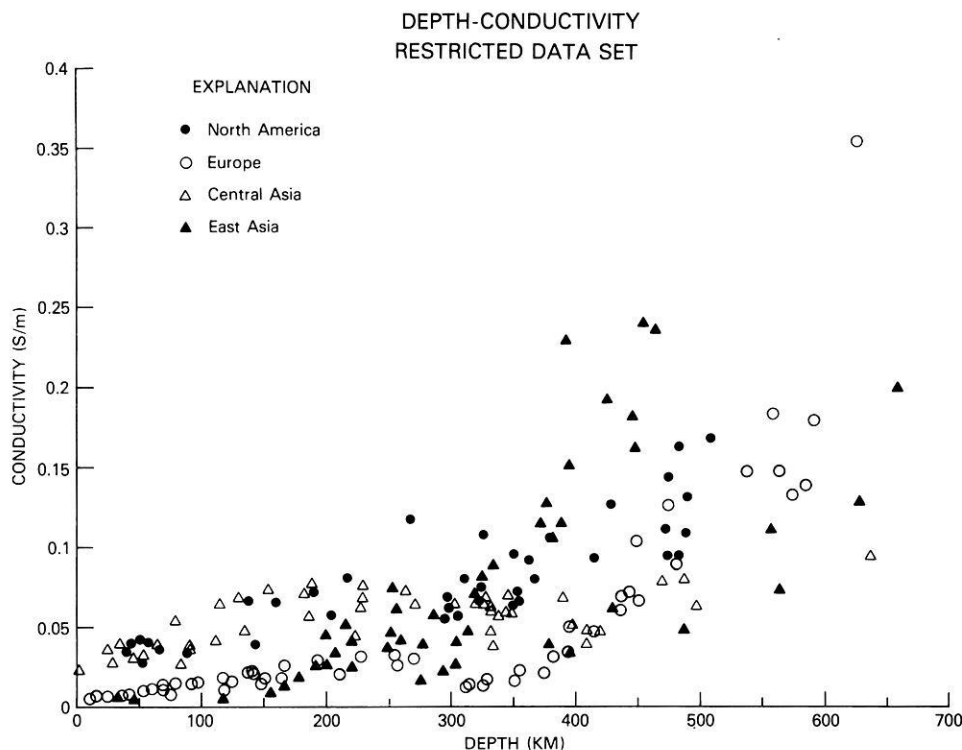


Fig. 5. Depth-conductivity values of Fig. 3, restricted by removal of the normal distribution tails about exponential curves given in Fig. 4. Separate groups represent North America, Europe, Central Asia and East Asia

there was an unknown mixture of contributions to the computations by the selected regional observatories.

Acknowledgements. We wish to thank Professor Schmucker of the University of Göttingen for his assistance in interpreting his effective-conductivity analysis method. We also thank the staff of World Data Center A for Solar Terrestrial Physics for providing magnetograms and for their stimulating scientific discussions.

References

- Anderson, D.L., Dziewonski, A.M.: Seismic tomography. *Sci. Am.*, **251**, 58–66, Oct. 1984
- Banks, R.J.: Geomagnetic variations and the electrical conductivity of the upper mantle. *Geophys. J. R. Astron. Soc.*, **17**, 457–487, 1969
- Campbell, W.H., Anderssen, R.S.: Conductivity of the subcontinental upper mantle: An analysis using quiet-day geomagnetic records of North America, *J. Geomagn. Geoelectr.*, **35**, 367–382, 1983
- Campbell, W.H., Schiffmacher, E.R.: Quiet ionospheric currents of the Northern Hemisphere derived from geomagnetic field records. *J. Geophys. Res.*, **90**, 6475–6486, 1985
- Chapman, S., Bartels, J.: *Geomagnetism*. Oxford: Clarendon Press, 1940
- Dziewonski, A.M., Anderson, D.L.: Preliminary reference earth model. *Phys. Earth Planet. Inter.*, **20**, 297–356, 1981
- Lahiri, B.N., Price, A.T.: Electromagnetic induction in non-uniform conductors and the conductivity of the earth from terrestrial magnetic variations. *Phil. Trans. R. Soc. London*, **A237**, 509–540, 1939
- Pollack, H.N., Chapman, D.S.: The flow of heat from the Earth's interior. *Seis. Am.* **237**, 60–76, 1977
- Schmucker, V.: An introduction to induction anomalies. *J. Geomagn. Geoelectr.*, **22**, 9–33, 1970
- Schmucker, V.: Erdmagnetische Variationen und die elektrische Leitfähigkeit in tieferen Schichten der Erde. *Sitzungsber. Mitt. Braunsch. Wiss. Ges.*, **4**, 45–102, 1979
- Shankland, T.J., Waff, H.S.: Partial melting and electrical conductivity anomalies in the upper mantle. *J. Geophys. Res.*, **82**, 5409–5417, 1977

Received March 8, 1985/Revised version July 17, 1985

Accepted July 31, 1985